IJC Heart & Vasculature 21 (2018) 22–28

Contents lists available at ScienceDirect

IJC Heart & Vasculature

journal homepage: http://www.journals.elsevier.com/ijc-heart-and-vasculature

Atrial fibrillation promotion in a rat model of heart failure induced by left ventricle radiofrequency ablation

Luis dos Santos [a,1], Ednei L. Antonio [a,1], Andrey J. Serra [b,1], Amanda Yoshizaki [a,1], Larissa Seibt [a,1], Flavio A. Silva [a,1], Gisele K. Couto [c,1], Luciana V. Rossoni [c,1], Paulo Tucci [a,1], Angelo A. de Paola [a,1], Guilherme Fenelon [a,*,1]

[a] Department of Cardiology, Paulista School of Medicine, Federal University of São Paulo, Rua Pedro de Toledo 781 10° - Vila Clementino, 04039-032 São Paulo, SP, Brazil
[b] Biophotonics Program, Nove de Julho University (UNINOVE), Rua Vergueiro, 235/249 - Vergueiro, 015 04000 São Paulo, SP, Brazil
[c] Department of Physiology and Biophysics, Institute of Biomedical Science, University of São Paulo, Av. Professor Lineu Prestes - 1524- Cidade Universitária, 05508-000 São Paulo, SP, Brazil

ARTICLE INFO

Article history:
Received 28 June 2018
Accepted 11 September 2018
Available online 22 September 2018

Keywords:
Radiofrequency ablation
Atrial fibrosis
Heart failure
Atrial fibrillation

ABSTRACT

Background: Atrial fibrillation (AF) frequently coexists with congestive heart failure (CHF). The increased susceptibility to AF in CHF has been attributed to a variety of structural and electrophysiological changes in the atria, particularly dilation and interstitial fibrosis. We evaluated atrial remodeling and AF vulnerability in a rat model of CHF induced by left ventricle (LV) radiofrequency (RF) ablation.

Methods: Wistar rats were divided into 3 groups: RF-induced CHF (Ab, n = 36), CHF animals treated with spironolactone (AbSpi, n = 20) and sham controls (Sham, n = 29). After 12 weeks, animals underwent echocardiographic and electrophysiological evaluation and were sacrificed for histological (atrial fibrosis) and Western blotting (TGF-β1, collagen I/III, connexin 43 and $Ca_V1.2$) analysis.

Results: Mild LV dysfunction and marked atrial enlargement were noted in both ablated groups. AF inducibility (episodes ≥2 s) increased in the Ab group compared to sham animals (31/36, 86%; vs. 15/29, 52%; p = 0.005), but did not differ from the AbSpi group (16/20, 80%; p = NS). Sustained AF (>30 s) was also more frequent in the Ab group compared to shams (56% vs. 28%; p = 0.04). Spironolactone reduced atrial fibrosis ($p < 0.01$) as well as TGF-β1 ($p < 0.01$) and collagen I/III ($p < 0.01$) expression but did not affect connexin 43 and $Ca_V1.2$ expression.

Conclusions: Rats with RF-induced CHF exhibit pronounced atrial structural remodeling and enhanced AF vulnerability. This model may be useful for studying AF substrate in CHF.

1. Introduction

Atrial fibrillation (AF) frequently coexists with congestive heart failure (CHF), as CHF promotes AF and as AF worsens CHF [1]. The increased susceptibility to AF in CHF has been attributed to a variety of structural and electrophysiological changes in the atria, particularly dilation and interstitial fibrosis [2]. Heart failure increases expression of transforming growth factor beta 1 (TGF-β1) which plays a significant role in the genesis of atrial fibrosis [3]. Furthermore, CHF is associated with decreased expression of connexins 40 and 43 (major atrial gap junctional proteins) [4,5]. These abnormalities promote slow local conduction favoring sustained reentry. In addition, heart failure-induced atrial remodeling is commonly associated with reduced expression of L-type Ca^{2+} channels which may change action potential configuration and atrial refractoriness [6]. It has been shown in animal models that mineralocorticoid receptor blockers such as spironolactone and eplerenone, which exhibit potent antifibrotic properties, attenuate CHF-induced atrial fibrosis and atrial tachyarrhythmias [1,7,8].

The rat model of myocardial infarction induced by ligation of the left coronary artery has long been validated to simulate human CHF and left atrial remodeling [9]. However, this model has drawbacks such as elevated significant immediate mortality and high variability of myocardial infarction size [10–11]. As an alternative to coronary occlusion, we have recently demonstrated a method of inducing myocardial infarction in rats by left ventricle radiofrequency (RF) ablation which is associated with homogenous infarct size and low mortality [12–14]. In addition, the histopathologic evolution, severity of left ventricular dysfunction and CHF outcome reproduced a myocardial infarction from coronary occlusion [12]. However, atrial structural alterations and AF susceptibility were not evaluated.

* Corresponding author.
E-mail address: guilhermefenelon@uol.com.br (G. Fenelon).
[1] This author takes responsibility for all aspects of the reliability and freedom from bias of the data presented and their discussed interpretation.

https://doi.org/10.1016/j.ijcha.2018.09.003

We hypothesized that our CHF model promotes left atrial dilation and interstitial fibrosis increasing vulnerability to AF. Therefore, we have assessed atrial structural remodeling and induction of AF in rats with CHF induced by RF ablation. Additionally, we evaluated the impact of spironolactone on atrial fibrosis and AF inducibility.

2. Methods

This study was approved by the Ethics in Research Committee of the Federal University of São Paulo (protocol number: 8052201213) and was conducted in accordance with "Laws related to animal models in Brazil" (http://www.ccs.ufpb.br/pesqccs/animal.htm).

2.1. Open-chest preparation and ablation protocol

Under sterile conditions, 85 male Wistar rats (300 to 320 g) were anesthetized, mechanically ventilated, and a thoracotomy in the 4th intercostal space was performed to expose the heart. One RF ablation (12 W for 12 s) per animal was performed on the free wall of the left ventricle using a customized catheter as previously described [12–14]. Then, the heart was rapidly placed back inside the thorax, and the chest was closed with simple suture. After recovery, animals were maintained for 12 weeks in conditioned cages in a light cycle of 12/12 h.

2.2. Subdivision of animals

Three groups were studied: (1) CHF induced by left-ventricle RF ablation (Ab group, n = 36); (2) CHF animals treated with spironolactone (100 mg/kg per gavage once daily) during the 12 weeks of follow-up (AbSpi group, n = 20); and (3) sham-operated animals (SHAM, n = 29) which underwent thoracotomy and exposure of the heart but not ablation.

At the end of the follow-up period (12 weeks), rats were reanesthetized for echocardiography and electrophysiological study. After that, animals were sacrificed, and the hearts excised for left atrial histological and Western blotting evaluation.

2.3. Echocardiography

Transthoracic echocardiography studies were performed using the HP SONOS 5500 echocardiograph (Philips Medical System, Andover, MA) with a 12 MHz transducer, 2 cm depth. In addition to left ventricular function analysis, left atrial diameter, area, and left atrial/aorta ratio were also evaluated as previously described [15].

2.4. Arrhythmia inducibility

Percutaneous electrophysiological studies were performed using an octapolar catheter (EPR catheter 1.6F, AD instruments) positioned in the right atrium via the right jugular vein [16]. Surface ECG and bipolar intracardiac electrograms (3 channels) were displayed on a monitor and stored by a computerized recording system (PowerLab®, Australia). Sinus node function and atrioventricular conduction intervals were not evaluated. Arrhythmia inducibility was tested with up to 5 burst pacing attempts at 20 and 40 milliseconds for a maximum of 30 s using current strengths from 1200 to 1500 mV (STG3008 stimulator, MultiChannels - Reutlingen, Germany). AF was defined as ≥2 s of irregular atrial electrogram (>800 bpm) with irregular ventricular response. AF episodes were categorized as follows: a) No AF induction (episodes <2 s); b) Non-sustained AF (≥2 s and ≤30 s); c) sustained AF (>30 second duration); d) sustained long-lasting AF (>15 minute–900 second duration). AF duration was measured from the end of the burst stimulus until the first P wave of sinus rhythm post-AF and was determined in each rat as the mean duration of all AF episodes.

2.5. Atrial refractoriness analysis

Due to poor catheter stability, we were not able to reliably assess right atrial refractory periods by extra-stimulus testing. Therefore, we used the AF cycle length recorded in the intracavitary electrodes as an estimate of atrial refractoriness [17–18]. The AF cycle length analysis consisted of manually measuring using electronic calipers (same blind observer) the atrial electrical activity intervals (averaging 10 to 20 cycles) during the 31st second of the AF episode of animals with sustained AF. We have chosen this time frame to allow accommodation of atrial refractoriness. The mean, median and shortest intervals of AF cycles were evaluated. AF displaying multicomponent fractionated electrograms or with motion artifacts were excluded.

2.6. Histology

Atrial fibrosis was quantified with Picrosirius red staining [19]. Quantitative analysis of collagen (measured in pixels) was performed after sequential images (10 fields per atrium) along the atrial fibers and blindly measured using Image Tool® software.

2.7. Western blotting

To determine protein expression of TGFβ1, collagen I/III, connexin 43 and L-type Ca^{2+} channels ($Ca_V1.2$) left atria were homogenized with cold RIPA lysis buffer (RIPA, Millipore, USA), containing phenylmethyl sulfonyl fluoride (PMSF, 1 mM), sodium orthovanadate (10 mM), protease inhibitor cocktail (2 μL/mL, Sigma, USA), sodium fluoride (100 mM) and sodium pyrophosphate (10 mM) [14]. The homogenates were subsequently centrifugated (1500g for 20 min at 4 °C) and the supernatants were isolated. Equal amounts of proteins (30 μg) of the samples, the molecular weight marker (Precision Plus Protein, Kaleidoscope, Bio-Rad, USA), and positive controls (30 μg of fibroblast homogenates as a positive control for collagen I/III, TGFβ1 and $Ca_V1.2$, and 30 μg of mouse encephalon homogenates as a positive control for connexin 43 were electrophoretically separated on gradient polyacrylamide gel (4–20%, Bio-Rad, USA) in an apparatus for minigel (Mini Protean III, Bio-Rad, USA) and transferred to polyvinylidene difluoride (PVDF) membranes (Amersham-GE Healthcare, UK) overnight at 4 °C using a Mini Trans-Blot Cell system (Bio-Rad, USA). After blocking, the membranes were incubated overnight at 4 °C with blocking solution containing the following antibodies: anti-collagen I/III (1:500; Calbiochem, California, USA, cat. n° 234169), anti-TGFβ1 (1:1000; Santa Cruz Biotechnology, Texas, USA, cat. n° sc-146), anti-connexin 43 (1:5000, Abcan, Massachusetts, USA, cat. n° ab11370) or anti-$Ca_V1.2$ (1:1000, Alomone Labs, Jerusalem, Israel, cat. n° ACC-003). After labeling with primary antibody, the membranes were incubated for 90 min with blocking solution containing appropriate peroxidase-conjugated secondary antibody (anti-rabbit; Jackson Immuno Research, USA): 1:10,000 for collagen I/III, 1:4000 for TGFβ1 and Connexin 43 or 1:2000 for $Ca_V1.2$. After washing, the fluorescence kit detection reagents (ECL, Amersham-GE Healthcare, UK) were added and the membrane chemiluminescence was detected using Amersham Imager 600 (Amersham-GE Healthcare, UK). Optical densitometric analysis of the bands was performed by the Image J program (Wayne Rasband, National Institutes of Health, USA). The loading control was validated by staining the membrane with Ponceau S.

2.8. Statistical analysis

Data were analyzed with the Prism 4.0 program (GraphPad Prism Software Inc., San Diego, CA, USA). The Fisher's exact test was used to compare AF inducibility. AF duration is expressed as median and interquartile range (25% to 75%) and was analyzed with a Kruskal-Wallis test followed by Dunn's test. Data normality was examined with Shapiro-Wilk test. One-way ANOVA was applied to compare continuous

variables among groups followed by Tukey's tests. Results are shown as mean ± standard deviation and significance level was set at $p \leq 0.05$.

3. Results

3.1. Radiofrequency ablation

The ablation procedure was uneventful in all animals, with no acute complications. However, during follow-up, mortality rate was 16% (n = 7/43) in the Ab group, 28% (n = 8/28) in the AbSpi group, and 17% (n = 6/35) in the sham group (p = NS). All deaths occurred during the first 3 weeks after ablation and were related to severe heart failure or surgical complications. In the sham group, half of the deaths was caused by unexpected pulmonary infection (these 3 rats were housed in the same cage). These animals were excluded from the analysis.

3.2. Echodopplercardiography

Twenty-nine animals in the sham group, 36 in the Ab group and 20 in the AbSpi group were evaluated by 2D echocardiography. Segmental contractile changes in the anterolateral wall, indicative of RF lesion, were observed in all ablated animals. In the Ab and AbSpi groups, respectively, there was dilation of the left ventricle (diastolic diameter 0.93 ± 0.10 cm vs. 0.95 ± 0.06 cm; p = NS) and mild reduction of LV ejection fraction (57 ± 11% vs. 52 ± 7%; p = NS). However, the degree of left atrium dilation was greater in the AbSpi group (0.69 ± 0.09 cm vs. 0.75 ± 0.06 cm; p = 0.02). In the sham group, left atrial diameter (0.62 ± 0.08 cm), left ventricle dimensions (diastolic diameter 0.73 ± 0.10 cm) and ejection fraction (83 ± 9%; p < 0.001) were normal and significantly different (p < 0.001) from ablated groups (Table 1).

3.3. Electrophysiological study

Twenty-nine animals in the sham group, 36 in the Ab group and 20 in the AbSpi group underwent electrophysiological evaluation. As shown in Fig. 1 (panels A and B), AF inducibility (episodes ≥2 s of duration) was significantly increased in the Ab group compared to sham animals (31/36, 86%; vs. 15/29, 52%; p = 0.005), but did not differ from the AbSpi group (16/20, 80%; p = NS). AF tended to be more easily induced in the AbSpi group than in sham animals (80% vs. 52%; p = 0.07). Sustained AF (>30 s of duration) was also induced more frequently in the Ab group compared to sham animals (20/36, 56%; vs. 8/29, 28%; p = 0.04), with no difference from the AbSpi group (7/20; 35%; p = NS). Inducibility of sustained AF did not vary between AbSpi and sham groups (35% vs. 28%; p = NS).

Table 1
Echocardiographic variables for ablation, ablation + spironolactone and sham groups 12 weeks after the ablation procedure.

Variable	SHAM (n = 29)	Ab (n = 36)	AbSpi (n = 20)
Body weight (g)	422.5 ± 50.89	435.4 ± 49.55	430.1 ± 34.46
LA(cm) - M mode	0.62 ± 0.08	0.69 ± 0.09**	0.75 ± 0.06***¥
ML (cm) 4-chamber view	0.53 ± 0.05	0.59 ± 0.09*	0.61 ± 0.08**
IS (cm) 4-chamber view	0.61 ± 0.07	0.69 ± 0.08***	0.73 ± 0.06***
LA area (cm^2) 4-chamber view	0.28 ± 0.05	0.36 ± 0.08***	0.38 ± 0.07***
LA area (cm^2) Bi-mode	0.42 ± 0.07	0.55 ± 0.13***	0.59 ± 0.19***
LA/Ao ratio Bi-mode	1.29 ± 0.18	1.62 ± 0.26***	1.7 ± 0.22***
LVDD (cm)	0.73 ± 0.10	0.93 ± 0.10***	0.95 ± 0.06***
LVSD (cm)	0.37 ± 0.17	0.68 ± 0.09***	0.72 ± 0.06***
Ejection fraction (%)	83 ± 8.9	57 ± 11***	52 ± 7.2***

Data described as mean ± standard deviation. Sham: sham group; Ab: ablation group; AbSpi: ablation treated with spironolactone group; LA: left atrium; ML: medial-lateral left atrium measured in the 4-chamber view; IS: inferior-superior left atrium measured in the 4-chamber view; LA/Ao: left atrium/aorta ratio measured by the short axis; LVDD: left ventricle diameter in diastole; LVDS: left ventricle diameter in systole; *p < 0.05; **p < 0.01; ***p < 0.001 versus SHAM; ¥p = 0.02 versus Ab.

Further, as illustrated in Fig. 1 (panel C), long lasting AF episodes (>15 min) occurred more frequently in the Ab group than in sham animals (12/36, 33% vs. 1/29, 3%; p = 0.004), but without difference as compared to the AbSpi group (5/20, 25%; p = NS). Long lasting AF was also more commonly induced in the AbSpi group than in sham animals (25% vs. 3%; p = 0.03).

Induced AF duration was not statistically different among the 3 study groups (p = 0.07), although there was a tendency toward increased AF duration in the Ab group compared with sham and AbSpi groups. AF duration in the AbSpi group was comparable to sham animals (Fig. 1, panel D).

The AF cycle length could be assessed in 7 animals (24%) from the sham group, 16 (44%) from the Ab group and 6 (30%) from the AbSpi group. Although recorded mean, median and shortest AF cycle length were longer in the Ab group (36 ± 13 ms; 36 ± 12 ms; 32 ± 12 ms) as compared to the AbSpi group (31 ± 3 ms; 31 ± 3 ms; 28 ± 4 ms) and sham animals (30 ± 4 ms; 30 ± 8 ms; 29 ± 4 ms), these differences were not significant.

3.4. Histology

Six animals in the sham group, 5 in the Ab group and 4 in the AbSpi group underwent histological evaluation. Left atrial interstitial fibrosis was increased in the Ab group as compared to sham animals (p < 0.001) and AbSpi group (p < 0.01). However, no differences in the amount of fibrosis were noted between AbSpi and sham rats (Fig. 2).

3.5. Western blotting

Four animals in each group were used for TGF-β1, collagen I/III and $Ca_V1.2$ expression analysis. Expression of TGF-β1 was significantly increased in left atria of the Ab group as compared to sham and AbSpi animals (p < 0.01), and collagen I/III also was significantly increased in the Ab group compared to sham and treated animals (p < 0.01). The treatment with spironolactone (AbSpi group) significantly reduced both TGF-β1 and collagen I/III protein expression in left atria to values comparable to those observed in intact animals. In ablated animals (Ab and AbSpi), $Ca_V1.2$ expression was significantly reduced as compared to sham animals (p < 0.01) with no difference between Ab and AbSpi groups. Expression of connexin 43 was evaluated in 5 animals from each group. In left atria from both ablated groups (Ab and AbSpi), expression of connexin 43 was significantly decreased as compared to sham animals (p < 0.01) and connexin 43 expression did not differ between Ab and AbSpi animals (Fig. 3).

4. Discussion

The present study is the first to examine atrial remodeling and AF arrhythmogenesis in our recently developed rat model of heart failure induced by left ventricle RF ablation [12–14]. We have demonstrated that rats with RF-induced heart failure exhibit marked atrial structural changes (dilation and interstitial fibrosis) and enhanced AF vulnerability compared to sham controls. Further, likewise other heart failure models, treatment with the mineralocorticoid receptor blocker spironolactone attenuated atrial fibrosis [3,19,20].

Our heart failure model was developed as an alternative to the rat model of myocardial infarction induced by ligation of the left coronary artery, which has long been validated to simulate human congestive heart failure and left atrial remodeling [9–11]. However, the coronary occlusion model is limited by its elevated immediate mortality (within 24 h), which varies between 13% to 65%, and high variability of left ventricle myocardial infarction size (40 ± 19%) [10–11]. Conversely, in our RF ablation model, immediate (24 h) mortality (7.5%) and myocardial infarction size dispersion (45 ± 8%; p = 0.001) are consistently lower compared with animals undergoing coronary occlusion [12–14]. Corroborating the

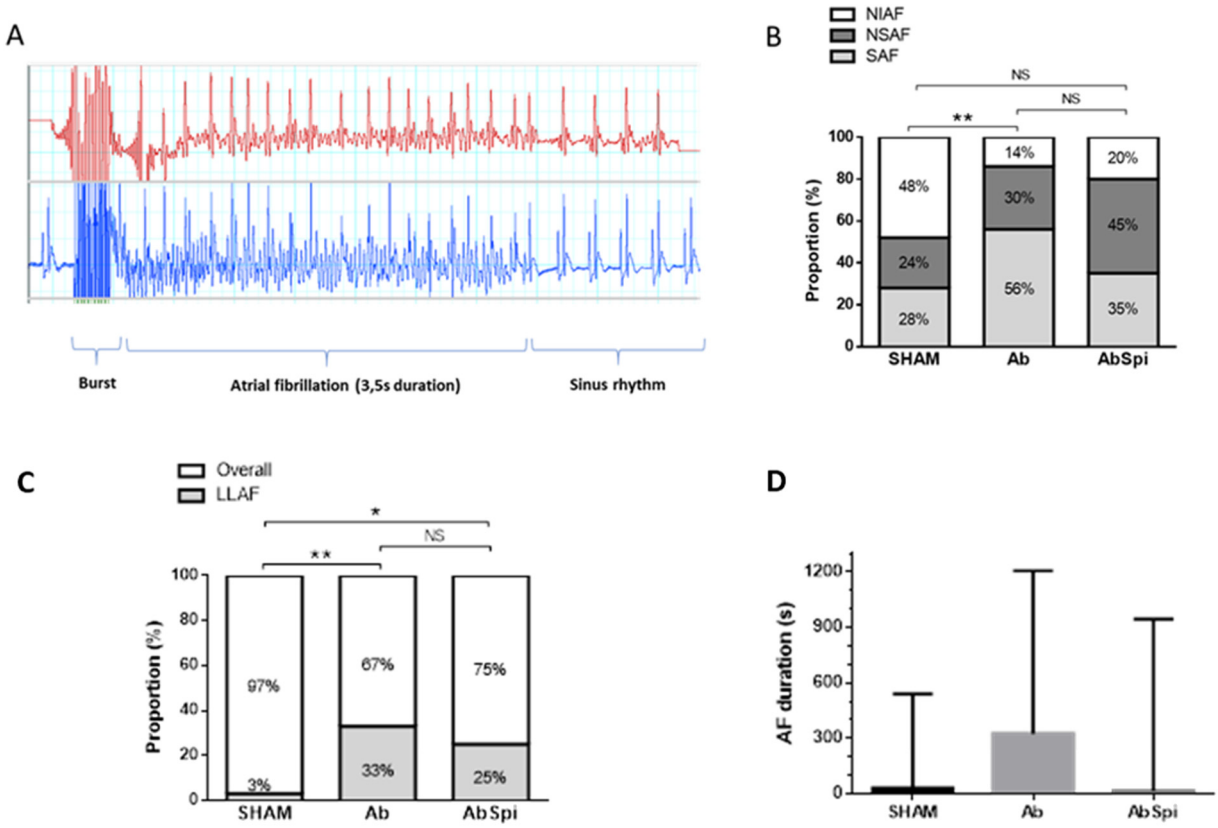

Fig. 1. (A) Atrial fibrillation (AF) induction (3.5 s duration) by a 30-millisecond burst pacing applied for 0.3 s. (B) AF inducibility rates for ablation (Ab), ablation + spironolactone (AbSpi) and sham groups. AF tended to be more easily induced in the AbSpi group than in sham animals ($p = 0.07$). (C) Long lasting (>15 min) atrial fibrillation (LLAF) inducibility rates for ablation (Ab), ablation + spironolactone (AbSpi) and sham groups. (D) AF duration. Data described as median and interquartile range. AF duration tended to be increased in the Ab group compared with sham and AbSpi groups ($p = 0.07$). NIAF: noninducible AF; NSAF: nonsustained AF; SAF: sustained AF; **$p = 0.005$ versus sham; NS: nonsignificant.

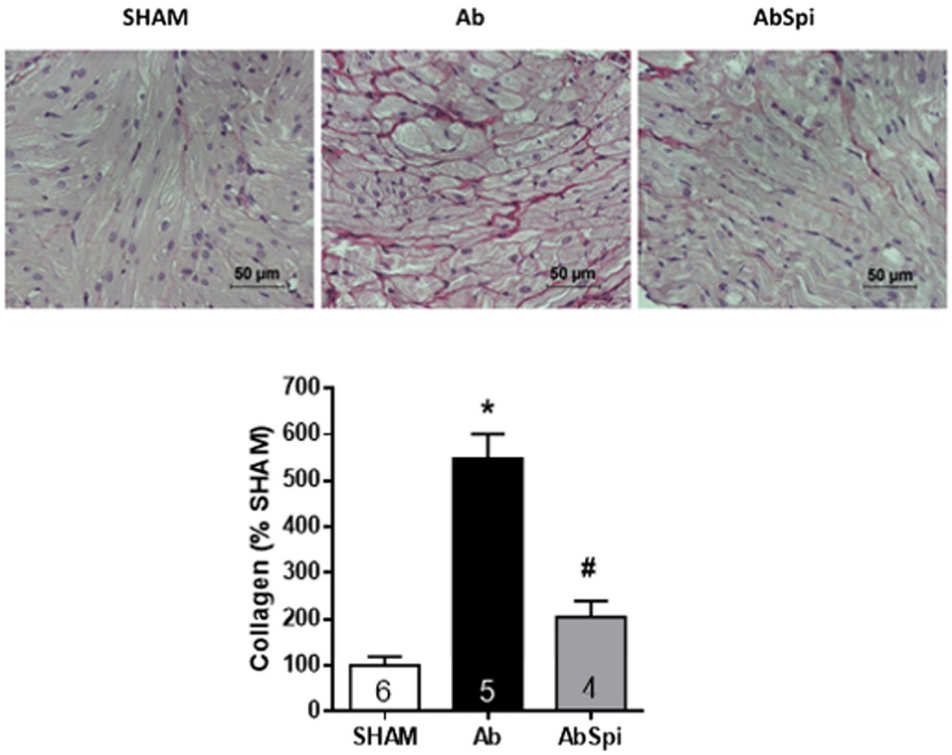

Fig. 2. Picrosirius stains of the left atrium from 1 animal in each group (top) and comparison of the percentage of collagen density in the left atrium (bottom). Interstitial fibrosis was increased in the ablation (Ab) group as compared to sham animals (*$p < 0.001$) and ablation + spironolactone (AbSpi) group (#$p < 0.01$). The amount of fibrosis did not differ between AbSpi and sham rats. Numbers inside bars indicate sample sizes.

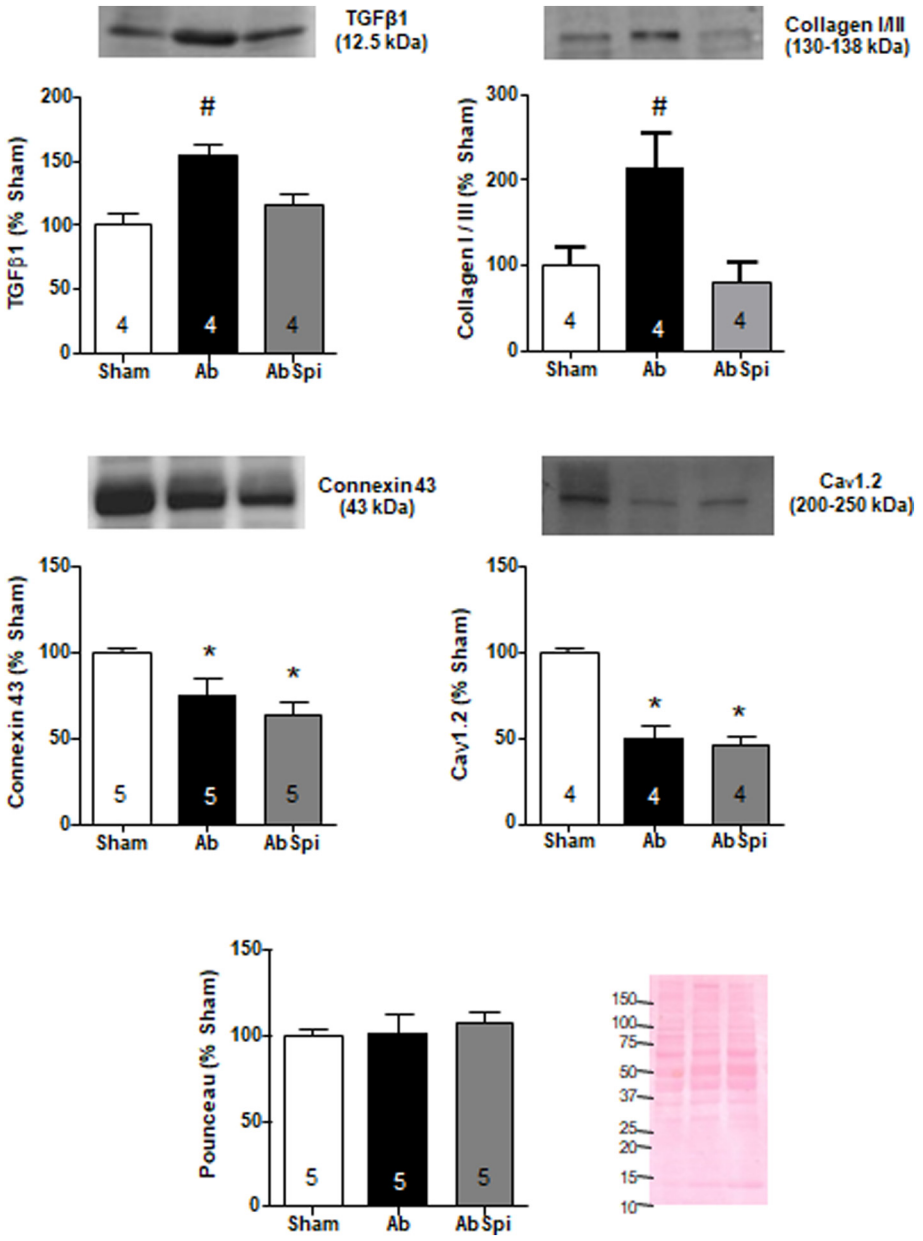

Fig. 3. Left atrial myocytes expression of: transforming growth factor beta 1 (TGFβ-1); collagen I/III; connexin 43; CaV1.2 and Ponceau staining as loading control for ablation (Ab), ablation + spironolactone (AbSpi) and sham groups. *p < 0.01 vs. sham; #p < 0.01 vs. sham and AbSpi groups. Numbers inside bars indicate sample sizes.

low mortality of our model, in the present study, death rate during the first 3 weeks of follow-up did not differ between ablated animals (Ab 16%, AbSpi 28%) and sham controls (17%; p = NS).

In our heart failure model induced by RF ablation, infarct size and the degree of myocardial dysfunction and atrial dilation are highly reproducible. These features derive from the mechanisms of RF lesion formation, which is thermally mediated and can be controlled by adjusting power delivery, application time and electrode size [11,12,21]. In the present study, ablated rats consistently developed mild heart failure and atrial remodeling, characterized by dilation and interstitial fibrosis of the left atrium (Table 1, Fig. 2). In addition, expression of the fibrogenic protein TGF-β1 and collagen I/III was markedly increased in the ablation group while gap junction protein connexin 43 and the L-type Ca^{2+} channel $Ca_v1.2$ were significantly decreased in ablated animals (Fig. 3). It is well recognized in animal models of heart failure that these structural abnormalities increase vulnerability to AF [1–3,22]. Accordingly, AF inducibility (episodes ≥2 s of duration) was consistently increased (Fig. 1B) in the ablation group compared to sham animals (86% vs. 52%; p = 0.005). Further, sustained (>30 s of duration) and long-lasting AF episodes (>15 min) were more frequently observed in the ablation group than in sham animals (Fig. 1, panels B and C). Of note, our AF inducibility rate (86%) is comparable to rats undergoing coronary occlusion (73%) [16,22].

It has been demonstrated in a rat model that aldosterone induces a substrate for atrial arrhythmias with locally disturbed conduction and characterized by atrial fibrosis and myocyte hypertrophy [23]. Noteworthy, these results were independent of increased atrial load pointing out to a direct proarrhythmic effect of aldosterone. Accordingly, it has been shown in experimental studies that mineralocorticoid receptor blockers mitigate heart failure-induced atrial fibrosis and AF inducibility [3,19,20,22]. In the present investigation, spironolactone significantly reduced atrial interstitial fibrosis as well as TGF-β1 and collagen I/III expression but did not affect connexin 43 and L-type Ca^{2+} channel $Ca_v1.2$ expression (Figs. 2 and 3), suggesting that changes in electrical remodeling represented by reduced $Ca_V1.2$ and connexin-43 expression are unchanged by spironolactone treatment. These observations further suggest that our RF ablation model exhibits atrial remodeling characteristics

comparable to those of heart failure induced by coronary occlusion [19,20,22]. Left atrial size was significantly larger in the spironolactone group compared to the ablation group (Table 1). The reasons for this finding are unclear but may be related to drug effects on atrial remodeling. Dilated left atrium is likely derived from left ventricular dysfunction and haemodynamic atrial overload [19]. Unfortunately, atrial pressure was not evaluated in our study.

Although aldosterone significantly reduced structural remodeling (less fibrosis) the AbSpi group exhibited almost the same inducibility of AF as the Ab group. This puzzling observation may be connected to persistent changes in the electrophysiological properties of the atrium (electrical remodeling) [2]. Expression of $Ca_v1.2$ and connexin 43 remained significantly decreased in animals treated with spironolactone. Atrial L-type Ca^{2+} current is downregulated in heart failure changing action potential configuration and refractoriness [2,6]. In addition, abnormal atrial Ca^{2+} handling occurs in heart failure [24,25] and other AF models like spontaneously hypertensive rats [26] and contribute to the development of ectopic activity. Accordingly, it is well recognized that AF can be initiated and maintained by rapid focal firing [2,22]. Finally, gap junction remodeling may promote slow local conduction favoring sustained reentry [2,4,5]. It has been consistently reported in animal models [4,5], including a rapid pacing pig model of AF and severe heart failure [27], that alterations in connexin 43 expression are associated with AF.

The increased susceptibility to AF in heart failure is mainly related to conduction abnormalities throughout the atria secondary to interstitial fibrosis [1–3]. Although atrial structural remodeling could be clearly demonstrated in our model, we were unable to determine the electrophysiological mechanisms underlying the increased AF vulnerability. Due to poor catheter stability, atrial refractory periods were not evaluated by extra-stimulus testing. As a result, we have used the AF cycle length recorded in the intracavitary electrodes as an estimate of atrial refractoriness [17,18]. AF intervals were longer in the ablation group than in sham animals, but this difference did not reach significance. Also, conduction velocity was not assessed. It would be interesting to conduct optical mapping studies to address these issues [28]. Nevertheless, AF vulnerability could be consistently demonstrated using a stimulation protocol with burst pacing for up to 30 s. This aggressive protocol could overestimate AF inducibility, but would not affect its sustenance. Furthermore, the definition of AF in our study required an arbitrary duration cut-off of at least 2 s whereas in most studies the duration cut-off ranges from 0.5 to 1.0 s [16,22,28]. Finally, atrioventricular conduction intervals were not recorded, but these variables do not affect AF inducibility.

4.1. Study limitations

This study was conducted in rats thus the results cannot be directly extrapolated to humans. Although AF vulnerability was increased, it is unclear whether spontaneous arrhythmias occur. The criteria used for measuring AF cycle length were arbitrary and subject to selection bias. Infarct size was not assessed, and the degree of left ventricular systolic dysfunction was determined by echocardiography only. Hemodynamic measurements were not performed, but they exhibit good correlations with echocardiography parameters [12]. Of note, our left ventricular ejection fraction figures for ablated and sham animals are comparable to other reports concerning infarcted rats and controls [29–32]. Mild systolic ventricular dysfunction was consistently induced in our model. Interestingly, in patients with mild systolic heart failure, eplerenone reduced the incidence of new onset atrial AF [33]. Because RF lesion formation can be easily controlled in the experimental setting [21], our model has the potential to titrate left ventricle lesion size reproducing several degrees of heart failure. Electrode-tissue contact force is a key factor in RF lesion size. Unfortunately, our custom catheter is not equipped with contact force sensing technology, which could further improve reproducibility of infarct size [34].

5. Conclusions

Rats with RF-induced mild heart failure exhibit pronounced atrial structural remodeling and enhanced AF vulnerability. These features reproduce those of heart failure induced by coronary occlusion. The low mortality and high reproducibility of left ventricle myocardial infarction size associated with our model make it attractive for studying AF substrate in heart failure.

Author contributions

Conceived and designed the experiments: LDS, PT, AADP, GF. Performed the experiments: LDS, ELA, AJS, AY, LS, FAS, GKC, LVR, GF. Analyzed the data: LDS, AJS, GKC, LVR, GF. Wrote the paper: LDS, LVR, GF.

Conflict of interest

There are no potential conflicts of interests.

Acknowledgements

This research was supported by grants (2013/23725-0; 2013/23553-5) from Fundação de Amparo à Pesquisa do Estado de São Paulo (LDS and GF).

References

[1] B.S. Stambler, K.R. Laurita, Atrial fibrillation in heart failure: steady progress but still a long way to go, Circ. Arrhythm Electrophysiol. 1 (2008) 77–79, https://doi.org/10.1161/CIRCEP.108.785071.
[2] S. Nattel, B. Burstein, D. Dobrev, Atrial remodeling and atrial fibrillation: mechanisms and implications, Circ. Arrhythm Electrophysiol. 1 (2008) 62–73, https://doi.org/10.1161/CIRCEP.107.754564.
[3] T.H. Everett 4th, J.E. Olgin, Atrial fibrosis and the mechanisms of atrial fibrillation, Heart Rhythm. 4 (2007) S24–S77, https://doi.org/10.1016/j.hrthm.2006.12.040.
[4] B. Burstein, P. Comtois, G. Michael, K. Nishida, L. Villeneuve, Y.H. Yeh, et al., Changes in connexin expression and the atrial fibrillation substrate in congestive heart failure, Circ. Res. 105 (2009) 1213–1222, https://doi.org/10.1161/CIRCRESAHA.108.183400.
[5] M.M. Jennings, J.K. Donahue, Connexin remodeling contributes to atrial fibrillation, J. Atrial Fibrillation 6 (2013) 839, https://doi.org/10.4022/jafib.839.
[6] R.C. Bond, S.M. Bryant, J.J. Watson, J.C. Hancox, C.H. Orchard, A.F. James, Reduced density and altered regulation of rat atrial L-type Ca^{2+} current in heart failure, Am. J. Physiol. Heart Circ. Physiol. 312 (2017) H384–H391, https://doi.org/10.1152/ajpheart.00528.2016.
[7] C. Lammers, T. Dartsch, M.C. Brandt, D. Rottländer, M. Halbach, G. Peinkofer, et al., Spironolactone prevents aldosterone induced increased duration of atrial fibrillation in rat, Cell. Physiol. Biochem. 29 (2012) 833–840, https://doi.org/10.1159/000178483.
[8] C. Tanaka-Esposito, S. Varahan, D. Jeyaraj, Y. Lu, B.S. Stambler, Eplerenone-mediated regression of electrical activation delays and myocardial fibrosis in heart failure, J. Cardiovasc. Electrophysiol. 25 (2014) 556–577, https://doi.org/10.1111/jce.12390.
[9] M.A. Pfeffer, J.M. Pfeffer, M.C. Fishbein, P.J. Fletcher, J. Spadaro, R.A. Kloner, et al., Myocardial infarct size and ventricular function in rats, Circ. Res. 44 (1979) 503–512, https://doi.org/10.1161/01.RES.44.4.503.
[10] C.F. Opitz, G.F. Mitchell, M.A. Pfeffer, J.M. Pfeffer, Arrhythmias and death after coronary artery occlusion in the rat: continuous telemetric ECG monitoring in conscious, untethered rats, Circulation 92 (1995) 253–261https://doi.org/10.1161/01.CIR.92.2.253.
[11] J.M. Pfeffer, M.A. Pfeffer, E. Braunwald, Influence of chronic captopril therapy on the infarcted left ventricle of the rat, Circ. Res. 57 (1985) 84–90https://doi.org/10.1161/01.RES.57.1.84.
[12] E.L. Antonio, A.A. dos Santos, S.R. Araujo, D.S. Bocalini, L. dos Santos, G. Fenelon, et al., Left ventricle radio-frequency ablation in the rat: a new model of heart failure due to myocardial infarction homogeneous in size and low in mortality, J. Card. Fail. 15 (2009) 540–548, https://doi.org/10.1016/j.cardfail.2009.01.007.
[13] L.F. dos Santos, E. Antonio, A. Serra, G. Venturini, M. Okada, S. Araújo, et al., Radiofrequency ablation does not induce apoptosis in the rat myocardium, Pacing Clin. Electrophysiol. 35 (2012) 449–455, https://doi.org/10.1111/j.1540-8159.2011.03306.x.
[14] L.F. dos Santos, E.L. Antonio, A.J. Serra, G. Venturini, J. Montemor, M. Okada, et al., Thermotolerance does not reduce the size or remodeling of radiofrequency lesions in the rat myocardium, J. Interv. Card. Electrophysiol. 36 (2013) 5–11, https://doi.org/10.1007/s10840-012-9746-6.
[15] R.M. Kanashiro, R.M. Saraiva, A. Alberta, E.L. Antonio, V.A. Moisés, P.J. Tucci, Immediate functional effects of left ventricular reduction: a Doppler echocardiographic study in the rat, J. Card. Fail. 12 (2006) 163–169 https://doi.org/10.1016/j.cardfail.2005.09.007.

[16] Y. Zhang, E. Dedkov, B. Lee, Y. Li, K. Pun, A.M. Gerdes, Thyroid hormone replacement therapy attenuates atrial remodeling and reduces atrial fibrillation inducibility in a rat myocardial infarction-heart failure model, J. Card. Fail. 20 (2014) 1012–1019, https://doi.org/10.1016/j.cardfail.2014.10.003.
[17] G. Fenelon, B.S. Stambler, E. Huvelle, P. Brugada, W.G. Stevenson, European VENTAK MINI Investigator Group, Left ventricular dysfunction is associated with prolonged average ventricular fibrillation cycle length in patients with implantable cardioverter defibrillators, J. Interv. Card. Electrophysiol. 7 (2002) 249–254 https://doi.org/10.1023/A:1021393525558.
[18] H.C. Yuen, S.Y. Roh, D.I. Lee, J. Ahn, D.H. Kim, J. Shim, et al., Atrial fibrillation cycle length as a predictor for the extent of substrate ablation, Europace 17 (2015) 1391–1401, https://doi.org/10.1093/europace/euu330.
[19] P. Milliez, N. Deangelis, C. Rucker-Martin, A. Leenhardt, E. Vicaut, E. Robidel, et al., Spironolactone reduces fibrosis of dilated atria during heart failure in rats with myocardial infarction, Eur. Heart J. 26 (2005) 2193–2199, https://doi.org/10.1093/eurheartj/ehi478.
[20] J. Zhao, J. Li, W. Li, Y. Li, H. Shan, Y. Gong, et al., Effects of spironolactone on atrial structural remodelling in a canine model of atrial fibrillation produced by prolonged atrial pacing, Br. J. Pharmacol. 159 (2010) 1584–1594, https://doi.org/10.1111/j.1476-5381.2009.00551.x.
[21] F.H. Wittkampf, H. Nakagawa, RF catheter ablation: lessons on lesions, Pacing Clin. Electrophysiol. 29 (2006) 1285–1297, https://doi.org/10.1111/j.1540-8159.2006.00533.x.
[22] K. Nishida, G. Michael, D. Dobrev, S. Nattel, Animal models for atrial fibrillation: clinical insights and scientific opportunities, Europace 12 (2010) 160–172, https://doi.org/10.1093/europace/eup328.
[23] J.C. Reil, M. Hohl, S. Selejan, P. Lipp, F. Drautz, A. Kazakow, et al., Aldosterone promotes atrial fibrillation, Eur. Heart J. 33 (2012) 2098–2108 https://doi.org/10.1093/eurheartj/ehr266.
[24] Y.H. Yeh, R. Wakili, X.Y. Qi, D. Chartier, P. Boknik, S. Kaab, et al., Calcium-handling abnormalities underlying atrial arrhythmogenesis and contractile dysfunction in dogs with congestive heart failure, Circ. Arrhythm Electrophysiol. 1 (2008) 93–102, https://doi.org/10.1161/CIRCEP.107.754788.
[25] P. Lugenbiel, F. Wenz, K. Govorov, P.A. Schweizer, H.A. Katus, D. Thomas, Atrial fibrillation complicated by heart failure induces distinct remodeling of calcium cycling proteins, PLoS One 10 (2015), e0116395. https://doi.org/10.1371/journal.pone.0116395.
[26] F. Pluteanu, J. Heß, J. Plackic, Preisenberger J. Nikonova, A. Bukowska, et al., Early subcellular Ca^{2+} remodelling and increased propensity for Ca^{2+} alternans in left atrial myocytes from hypertensive rats, Cardiovasc. Res. 106 (2015) 87–97, https://doi.org/10.1093/cvr/cvv045.
[27] T. Igarashi, J.E. Finet, A. Takeuchi, Y. Fujino, M. Strom, I.D. Greener, et al., Connexin gene transfer preserves conduction velocity and prevents atrial fibrillation, Circulation 125 (2012) 216–225, https://doi.org/10.1161/CIRCULATIONAHA.111.053272.
[28] Y.K. Iwasaki, T. Kato, F. Xiong, Y.F. Shi, P. Naud, A. Maguy, et al., Atrial fibrillation promotion with long-term repetitive obstructive sleep apnea in a rat model, J. Am. Coll. Cardiol. 64 (2014) 2013–2023, https://doi.org/10.1016/j.jacc.2014.05.077.
[29] A.B. Stein, S. Tiwari, P. Thomas, G. Hunt, C. Levent, M.F. Stoddard, et al., Effects of anesthesia on echocardiographic assessment of left ventricular structure and function in rats, Basic Res. Cardiol. 102 (2007) 28–41 https://doi.org/10.1007/s00395-006-0627-y.
[30] E. Guasch, B. Benito, X. Qi, C. Cifelli, P. Naud, Y. Shi, et al., Atrial fibrillation promotion by endurance exercise: demonstration and mechanistic exploration in an animal model, J. Am. Coll. Cardiol. 62 (2013) 68–77, https://doi.org/10.1016/j.jacc.2013.01.091.
[31] K.I. Cho, S.H. Koo, T.J. Cha, J.H. Heo, H.S. Kim, G.B. Jo, et al., Simvastatin attenuates the oxidative stress, endothelial thrombogenicity and the inducibility of atrial fibrillation in a rat model of ischemic heart failure, Int. J. Mol. Sci. 15 (2014) 14803–14818, https://doi.org/10.3390/ijms150814803.
[32] R.C. Pasqualin, C.T. Mostarda, L.E. de Souza, M.F. Vane, R. Sirvente, D.A. Otsuki, et al., Sevoflurane preconditioning during myocardial ischemia-reperfusion reduces infarct size and preserves autonomic control of circulation in rats, Acta Cir. Bras. 31 (2016) 338–345 https://doi.org/10.1590/S0102-865020160050000008.
[33] K. Swedberg, F. Zannad, J.J. McMurray, H. Krum, D.J. van Veldhuisen, H. Shi, et al., EMPHASIS-HF Study Investigators, Eplerenone and atrial fibrillation in mild systolic heart failure: results from the EMPHASIS-HF (Eplerenone in Mild Patients Hospitalization And SurvIval Study in Heart Failure) study, J. Am. Coll. Cardiol. 59 (2012) 1598–1603, https://doi.org/10.1016/j.jacc.2011.11.063.
[34] A. Ikeda, H. Nakagawa, H. Lambert, D.C. Shah, E. Fonck, A. Yulzari, et al., Relationship between catheter contact force and radiofrequency lesion size and incidence of steam pop in the beating canine heart: electrogram amplitude, impedance, and electrode temperature are poor predictors of electrode-tissue contact force and lesion size, Circ Arrhythm Electrophysiol 7 (2014) 1174–1180, https://doi.org/10.1161/CIRCEP.113.001094.